crystals

MDPI

Article

Research on Ultrasonic-Assistance Microarc Plasma Polishing Method for 4H-SiC

Feilong Liu, Jiayi Yue, Jianhua Shi, Shujuan Li, Yanfei Zhang and Zhenchao Yang *

School of Mechanical and Precision Instrument Engineering, Xi'an University of Technology, Xi'an 710048, China; 105071@xaut.edu.cn (F.L.); 1240210009@stu.xaut.edu.cn (J.Y.); shijianhua0831@163.com (J.S.); shujuanli@xaut.edu.cn (S.L.); yfzhang@xaut.edu.cn (Y.Z.)

* Correspondence: zcyang@xaut.edu.cn

Abstract

Silicon carbide (SiC) is widely used in high-power, high-frequency, and high-temperature electronic devices due to its excellent physical and chemical properties. However, its high hardness and chemical inertness make it difficult to achieve efficient and damage-free ultra-smooth surface processing with traditional polishing methods. This paper proposes a novel ultrasonic-assistance microarc plasma polishing (UMPP) method for high-quality and high-efficiency polishing of 4H-SiC. This study introduces a novel Ultrasonic-assisted Microarc Plasma Polishing (UMPP) method for achieving high-efficiency, high-quality surface finishing of 4H-SiC. The technique innovatively combines ultrasonic vibration with microarc plasma oxidation in a neutral NaCl electrolyte to overcome the limitations of conventional polishing methods. The UMPP process first generates a soft, porous oxide layer (primarily SiO_2) on the SiC surface through plasma discharge, which is then gently removed using soft CeO_2 abrasives. The key finding is that ultrasonic assistance synergistically enhances the oxidation process, leading to a thicker and more porous oxide layer that is more easily removed. Experimental results demonstrate that UMPP achieves a remarkably high material removal rate (MRR) of 21.7 μm/h while simultaneously delivering an ultra-smooth surface with a roughness (Ra) of 0.54 nm. Compared to the process without ultrasonic assistance, UMPP provides a 21.9% increase in MRR and a 28% reduction in Ra. This work establishes UMPP as a highly promising and efficient polishing strategy for hard and inert materials like SiC, offering a superior combination of speed and surface quality that is difficult to achieve with existing techniques.

Keywords: silicon carbide; ultrasonic; microarc plasma; polishing; oxidation; material removal rate; surface roughness

check for updates

Academic Editor: Dmitri Donetski

Received: 25 September 2025
Revised: 14 October 2025
Accepted: 15 October 2025
Published: 17 October 2025

Citation: Liu, F.; Yue, J.; Shi, J.; Li, S.; Zhang, Y.; Yang, Z. Research on Ultrasonic-Assistance Microarc Plasma Polishing Method for 4H-SiC. *Crystals* **2025**, *15*, 902. https://doi.org/10.3390/cryst15100902

Copyright: © 2025 by the authors. Licensee MDPI, Basel, Switzerland. This article is an open access article distributed under the terms and conditions of the Creative Commons Attribution (CC BY) license (https://creativecommons.org/licenses/by/4.0/).

1. Introduction

Silicon carbide (SiC), particularly the 4H-SiC polytype, has garnered significant attention as a promising semiconductor material for high-power, high-frequency, and high-temperature electronic devices due to its exceptional physical and chemical properties. However, the extreme hardness and chemical inertness of SiC pose considerable challenges in achieving ultra-smooth, damage-free surfaces through conventional polishing techniques, which are critical for device performance and reliability.

Recent advances in polishing technologies have focused on enhancing both the material removal rate (MRR) and surface quality by integrating chemical and mechanical processes. Various innovative approaches have been developed, including photocatalytic

fixed polishing plates [1], electrochemical mechanical polishing (ECMP) [2], Fenton-assisted polishing [3], shear-thickening polishing (STP) [4], and photo-electrochemical mechanical polishing (PECMP) [5]. These methods leverage synergistic effects between chemical reactions, which lead to the oxidation of the SiC, and mechanical abrasion, which aims to remove the oxidation layer to improve polishing efficiency and surface integrity.

For instance, Li et al. [6] proposed a chemical–mechanical polishing method using multi-catalyst synergistic activation of potassium peroxymonosulfate, achieving a high MRR of 2360 nm/h. However, the resulting surface roughness Ra of 8.251 nm is relatively high for applications requiring ultra-smooth surfaces. In contrast, Wang et al. [2] optimized the SiC-ECMP process to achieve an exceptionally smooth surface with Ra of 0.287 nm, but the associated MRR of 2.32 μm/h may be insufficient for high-throughput manufacturing. Lin et al. [1] utilized a TiO_2-based photocatalytic fixed polishing plate to achieve an MRR of 4.05 μm/h and a surface roughness Ra of 1.09 nm on single-crystal SiC. Similarly, while Kang et al. [3] reported that Fenton-electrochemical oxidation nearly quadrupled the MRR compared to conventional CMP and achieved an ultra-smooth surface (Ra = 0.127 nm), their method relies on specific chemical agents like Fenton's reagent, which can introduce complexity in waste treatment. Other studies, such as shear-thickening polishing (STP) [4] or electrochemical shear-thickening polishing (ESTP) [5], demonstrate excellent results but often involve complex setups or slurry systems.

Moreover, the role of dispersants in stabilizing polishing slurries [7], the application of solid-phase catalysts like GO/Fe_3O_4 [8], and the use of molecular dynamics simulations to unravel atomic-scale mechanisms [9] have provided deeper insights into the polishing processes and enabled more precise control over surface finishing.

Furthermore, the role of ultrasonic vibration in improving the polishing quality and efficiency of SiC has been previously established. For instance, ultrasonic energy has been integrated into Chemical Mechanical Polishing (CMP) to enhance slurry transport and material removal, as shown in studies of ultrasonic CMP combined with ultrasonic lapping [10] and ultrasonic chemical assisted polishing [11]. Similarly, ultrasonic vibration has been applied in machining processes like mill-grinding to improve the machinability of SiC [12]. More recent studies have further explored the coupling of ultrasound with catalytic reactions and its synergistic effect with hydroxyl radicals to enhance the chemical component of polishing SiC [13] and SiC ceramics [14].

Meanwhile, microarc plasma oxidation (MPO) is an established electrochemical surface treatment process used in alloy parts, at present, under the condition of high voltage and environmental saline solution. Its fundamental plasma formation mechanisms have been extensively studied, as detailed in works like that of Mi et al. [15]. The primary application of MPO has traditionally been the synthesis of functional ceramic coatings on valve metals such as titanium [16] and zirconium [17] to enhance properties like surface hardness, wear resistance, and bioactivity. However, this established body of knowledge is almost exclusively confined to the domain of metallurgy and surface engineering for protective coating purposes.

In summary, while the prevailing paradigm for SiC polishing effectively relies on a two-step "oxidation-removal" mechanism, these methods face inherent limitations. The chemical oxidation steps (photocatalytic, Fenton, electrochemical, etc.) are often rate-limiting, constraining the maximum achievable Material Removal Rate (MRR). Furthermore, achieving a high MRR frequently comes at the cost of surface quality, as seen in methods that prioritize speed but result in higher roughness, or vice versa. There exists a critical need for a rapid oxidation technique that can simultaneously deliver both high efficiency and superior surface integrity.

Interestingly, a highly efficient oxidation technology exists in a parallel field: Microarc Plasma Oxidation (MPO). MPO is a well-established process for growing robust oxide coatings on metals like titanium and zirconium in environmental saline solutions, leveraging intense, localized plasma discharges to achieve high oxidation rates. However, its potential has been confined solely to protective coating applications in metallurgy, and its application to the high-rate, precision polishing of semiconductors like SiC remains virtually unexplored.

This work bridges this technological divide. The paper proposes that the high-energy plasma discharges of MPO can be harnessed not only for coating, but also for the ultra-efficient surface modification of SiC. By adapting MPO as a rapid oxidation step, the Ultrasonic-assisted Microarc Plasma Polishing (UMPP) method is introduced, aiming to overcome the oxidation rate bottleneck of existing methods and achieve a superior combination of high MRR and low surface roughness. Thus, a flat surface without surface defects is expected with the application of UMPP. Furthermore, the oxidation mechanism of UMPP is discussed.

2. Mechanism of UMPP

This method mainly consists of two steps:

1. The ultrasonic-assistance microarc plasma oxidation (UMPO) process on the surface of single-crystal SiC, as shown in Figure 1.
2. The mechanical removal of the oxide film by soft abrasive particles. In this polishing method, the ultrasonic-assistance microarc plasma oxidation process on the surface of 4H-SiC is the core, which determines the polishing efficiency (material removal rate, MRR) and the surface quality after polishing (surface roughness, Ra).

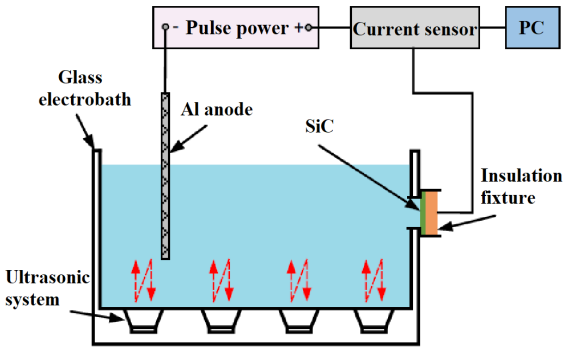


Figure 1. Ultrasonic-assistance Microarc Plasma Oxidation of 4H-SiC.

2.1. Macroscopic Mechanism of Microarc Plasma Oxidation of 4H-SiC

In the microarc plasma oxidation system, the single crystal SiC (anode) and the metal electrode (cathode) are immersed in the electrolyte and connected to a high-frequency pulse power supply. Initially, both electrodes are in direct, unimpeded contact with the NaCl electrolyte, forming a complete electrical circuit with low initial impedance. When the high voltage is applied, a large initial current flows, causing the electrolyte at the electrode interfaces to heat up rapidly via Joule heating. This heat instantly vaporizes the surrounding electrolyte, forming a stable gas layer that subsequently insulates the SiC anode from the liquid electrolyte. When the external electric field strength increases and reaches the breakdown threshold of the gas medium, the gas layer will be broken down and form a certain conductive plasma channel. There will be intense gas discharge and chemical reactions between the surface of the SiC and the plasma gas layer, and the surface of the SiC in contact with the gas layer will be oxidized. The macroscopic mechanism diagram of the microarc plasma oxidation of SiC is shown in Figure 2.

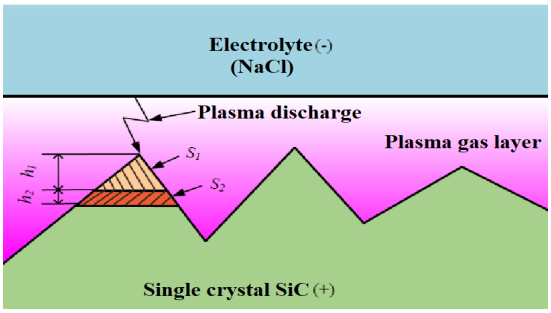


Figure 2. Macroscopic mechanism of UMPO.

The oxidation reaction initially occurs at the peak points where the thickness of the plasma gas layer is relatively thin, causing the protrusions on the surface of the SiC to be oxidized preferentially. This preferential oxidation at surface protrusions is the fundamental mechanism enabling surface flattening. Because the electric field is enhanced at sharp peaks, the plasma discharges target these high points first. The process converts a taller, sharper peak of hard SiC into a broader, shallower mound of soft oxide. During the subsequent mechanical polishing step, this softer, more voluminous oxide on the high points is removed more easily than the untouched SiC in the valleys. This selective modification and removal of high points iteratively reduce the height difference between peaks and valleys, leading to global planarization of the surface. The diagram illustrates that, for the same amount of material oxidized ($S_1 = S_2$), the vertical thickness of the oxide layer (h) is less on a peak than in a valley. This means that multiple discharge cycles will progressively reduce the peak's height more rapidly than they deepen the valley, further contributing to flattening.

2.2. Microcosmic Mechanism of Microarc Plasma Oxidation

Figure 3 is the schematic diagram illustrating the microscopic mechanism of microarc plasma oxidation of 4H-SiC.

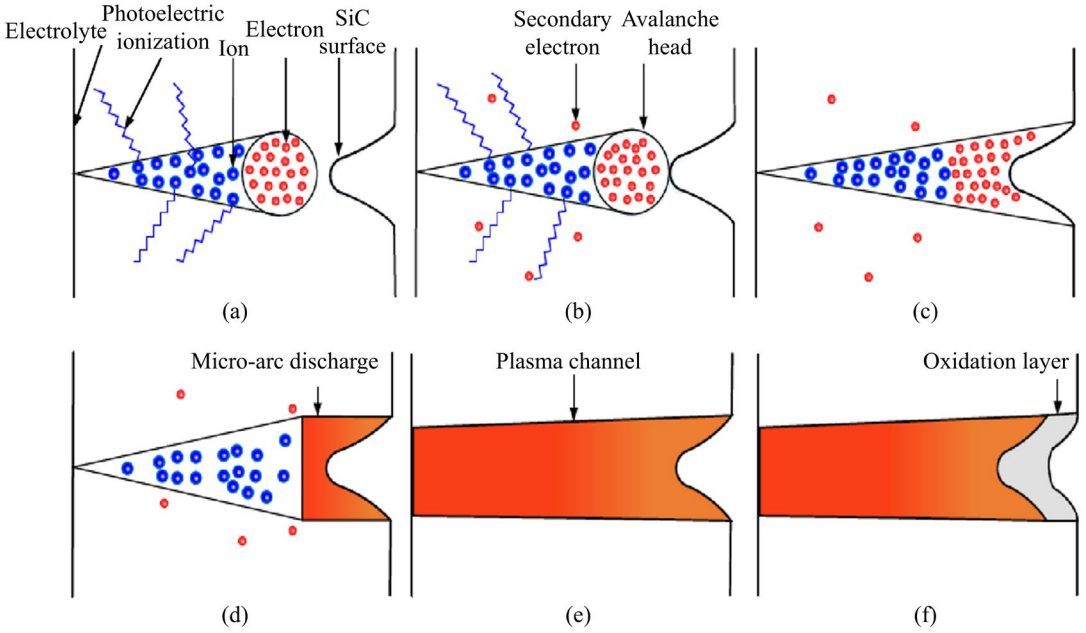


Figure 3. Microcosmic mechanism of microarc plasma oxidation. (**a**) Formation of the main electron avalanche. (**b**) Development of the electron avalanche. (**c**) Electron arrival at anode. (**d**) Incomplete discharge channel. (**e**) Formation of complete discharge channel. (**f**) Oxidization of the anode surface.

The 4H-SiC and the metal electrode are, respectively, connected to the positive and negative terminals of the pulse power supply. When the circuit is closed, the water molecules in the electrolyte undergo an ionization reaction first:

$$H_2O \rightarrow H^+ + OH^- \quad (1)$$

According to electrochemical theory, OH^- is more prone to discharge than other anions in the system. Therefore, the OH^- near the anode loses electrons first to produce oxygen, and the reaction equation is:

$$4OH^- - 4e^- \rightarrow 2H_2O + O_2 \quad (2)$$

Therefore, a certain number of electrons will accumulate in the electrolyte in contact with the SiC surface. Due to the generation of a large amount of heat on the surface, the surrounding electrolyte evaporates and forms a gas layer mainly composed of water vapor, which separates the electrolyte from the workpiece. At this time, the electrons accumulated on the surface of the electrolyte will move rapidly towards the surface of the SiC under the action of a high electric field. During the movement of electrons, they will inevitably collide with the surrounding gas molecules and generate new electrons and ions, eventually forming a main electron avalanche accompanied by light radiation, as shown in Figure 3a. The main electron avalanche in the discharge space can occur at any point [18]. Along with the generation of the main electron avalanche, photoelectrons are also emitted, and secondary ionization occurs. The electrons generated by secondary ionization still move rapidly towards the anode, creating a new electron bubble with a smaller size, as shown in Figure 3b. In Figure 3c, when the front end of the main electron avalanche contacts the surface of the anode workpiece, a large number of positive ions gathered near the anode cause an electric field distortion and attract the secondary ionization-generated secondary electron avalanche to form an incomplete discharge channel (Figure 3d). When more secondary electron avalanches are attracted to the vicinity of the anode, the discharge channel will rapidly develop towards the cathode until a complete discharge channel with a high density of charged particles is formed, as shown in Figure 3e.

During the discharge process, a large number of highly oxidizing hydroxyl radicals (•OH) will be generated:

$$2H_2O \rightarrow 2\bullet OH + 2H^+ + 2e^- \quad (3)$$

$$OH^- + h^+ \rightarrow \bullet OH \quad (4)$$

The generated hydroxyl radicals, under the action of an electric field, travel along the discharge channel to the surface of the SiC and undergo an oxidation reaction with it to form an oxide layer as shown in Figure 3f. The reaction process is as follows:

$$SiC + 4\bullet OH + O_2 \rightarrow SiO_2 + 2H_2O + CO_2 \uparrow \quad (5)$$

$$SiC + 4h^+ + 4\bullet OH \rightarrow SiO + 2H_2O + CO \uparrow \quad (6)$$

The thickness of the gas layer is smaller at the protruding areas on the surface of the SiC, and the local electric field intensity is high. Therefore, the electrons on the electrolyte surface reach these protruding positions faster and with a shorter distance, entering the anode earlier and forming discharge channels preferentially at these positions. Meanwhile, the probability of forming discharge channels at the concave areas is lower than that at the protruding areas, resulting in the priority of reaching the protruding areas being oxidized more quickly. This is the key to achieving a flat surface after the oxide layer's removal.

2.3. The Influence Mechanism of Ultrasonic Vibration on the Oxidation Process

The ultrasonic vibration emitted by the ultrasonic units propagates in the electrolyte, generating an ultrasonic effect, which promotes the heating of the electrolyte, causes cavitation and chemical effects, thereby further increasing the oxidation rate of the 4H-SiC surface.

1. The heating effects

In the ultrasonic-assistance microarc plasma oxidation system, ultrasonic energy is dissipated as heat within the electrolyte, raising its bulk temperature. This temperature increase has several consequential effects that enhance the plasma oxidation process:

Enhanced Ionic Mobility: A higher electrolyte temperature reduces the fluid's viscosity and increases ionic mobility. This facilitates the transport of charge carriers (e.g., OH^-, NA^+) to the reaction interface, replenishing the species consumed during plasma discharge and sustaining the electrochemical reactions that underpin the oxidation process.

Lower Enthalpy of Vaporization: The energy required to form and maintain the vapor gas layer (VGL) is reduced at higher temperatures. This means a greater proportion of the discharge energy can be directed toward heating the SiC substrate and driving the oxidation reaction, rather than being consumed by vaporizing the electrolyte.

Increased Molecular Entropy: As noted by the authors, the thermal energy increases the kinetic energy of molecules and ions. These more energetic particles are more likely to overcome solvation forces and enter the gas phase, thereby increasing the density of particles available to be ionized within the discharge channel. This directly intensifies the plasma discharge and increases the frequency of discharge events.

Therefore, the primary effect of ultrasonic heating is to create a more active and responsive electrochemical environment that promotes more intense and frequent plasma discharges, thereby increasing the overall oxidation rate of the SiC surface.

2. The cavitation effects

The cavitation effect of ultrasonic vibration accelerates the renewal and flowing of the electrolyte, improves the flow field, enhances the activity of the SiC surface, and promotes the electrochemical reactions. At the same time, the high pressure, shock waves and micro jets generated by ultrasonic cavitation increase the strain degree on the SiC surface. Due to the promoting effect of surface strain, the oxidation of the strain area becomes easier, thereby increasing the oxidation rate of the SiC surface.

3. The chemical effects

During the ultrasonic cavitation process, the bubble collapse generates local hotspots, which have extremely high temperatures and pressures. Within a few microseconds, these hotspots thermally decompose water vapor into free radicals, accompanied by the generation of shock waves. They possess strong oxidizing properties and can oxidize the SiC. The reaction process is as follows:

$$H_2O \rightarrow \bullet H + \bullet OH \quad (7)$$

$$\bullet H + \bullet H \rightarrow H_2 \uparrow \quad (8)$$

$$\bullet OH + \bullet OH \rightarrow H_2O_2 \quad (9)$$

$$\bullet H + \bullet OH \rightarrow H_2O \quad (10)$$

$$SiC + 8\bullet OH + O_2 \rightarrow SiO_2 + 4H_2O + CO_2 \uparrow \quad (11)$$

The electron with the smallest mass is most likely to undergo acceleration under the action of ultrasonic energy. The accelerated electrons collide with water vapor molecules in

the gas film, generating more secondary electrons, which intensifies the electron avalanche and enhances the plasma density in the conductive channel. At the same time, a large number of high-energy electrons undergo inelastic collisions with water vapor molecules. The ultrasonic vibration can accelerate the generation rate of hydroxyl radicals (•OH), and the high concentration of hydroxyl radicals (•OH) accelerates the oxidation of the SiC surface.

The instantaneous high pressure generated by the ultrasonic vibration, along with the continuous formation of hydroxyl radicals (•OH) and the enhanced fluidity of the electrolyte, all contribute to increasing the oxidation rate of the SiC. The ultrasonic vibration can activate the SiC surface, increasing the number of electron–hole pairs on the SiC surface. The electron–hole pairs promote the generation of hydroxyl radicals (•OH) and thereby improve the oxidation efficiency of the SiC.

3. Experiment Setup

As shown in Figure 4, in the ultrasonic-assistance microarc plasma oxidation system, the Al plate was connected to the negative electrode of the power supply as the cathode, and the SiC wafer connected to the positive electrode of the power supply was fixed in a 10 mm diameter wall hole on the right side of the glass electrolytic cell, 80 mm away from the bottom of the cell, and was fixed with an insulating fixture for the workpiece. The electrolyte for each experiment did not reach the upper edge of the wall hole. The power supply was a single-polarity high-frequency pulse power supply independently developed by our team (model JCL-DSP3) [19], with a power of 3 kW, adjustable current range of 0 to 10 A, adjustable frequency range of 100 Hz to 100 kHz, and duty cycle range of 10% to 80%. The current data acquisition system consists of a Hall closed-loop current sensor, acquisition instrument, and computer. The Hall closed-loop current sensor was JLB-13 (JINGLIANG ELECTRONICS (Wuhan, China)), with a rated input current of 10 A and a response time of 1 μs. The acquisition instrument was NI 9232 (Emerson (Shanghai, China)), with a sampling frequency of 100 kHz. The ultrasonic frequency of 28 kHz and power of 300 W were identified as optimal through preliminary scoping experiments. A frequency range of 20–40 kHz and a power range of 150–450 was evaluated and found that 28 kHz and 300 W yielded the highest material removal rate without introducing surface damage from overly intense cavitation. The electrolytic cell in the microarc plasma oxidation system is immersed in a water tank, which is convenient for observing the ultrasonic vibration.

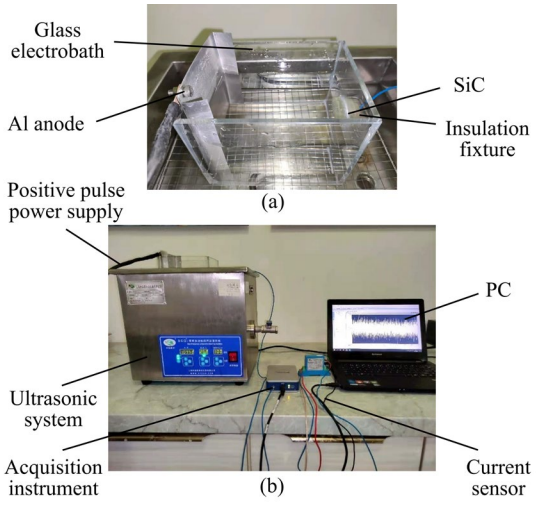


Figure 4. Ultrasonic-assistance microarc plasma oxidation system. (**a**) Electrobath details. (**b**) The whole device.

The mechanical polishing system used in this study is a reciprocating direct-push gravity-type grinding and polishing machine, as shown in Figure 5. The polyurethane polishing pad is fixed on the cast iron polishing disc through its back adhesive. The oxidized SiC wafer is fixed on the loading block with the help of a special bonding wax, and the loading block is placed in the adjustment disc. When the polishing surface comes into contact with the polishing pad and undergoes relative motion, the loading block's own gravity exerts downward pressure on the workpiece, and the abrasive particles in the polishing liquid can remove the oxide layer.

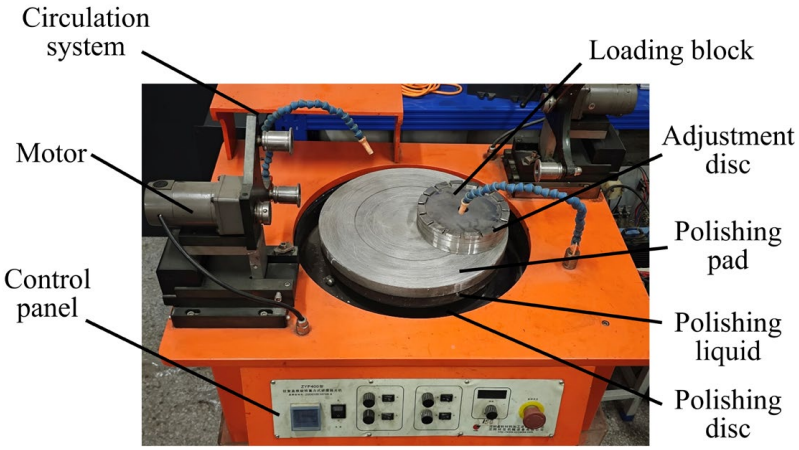


Figure 5. Mechanical Polishing System.

The wall holes on the side of the electrolytic cell for holding the workpiece have a diameter of 10 mm. Therefore, the 4H-SiC workpiece needs to be cut into specimens with dimensions of 13 mm × 13 mm. Before the experiment, the cut specimens need to be chemically cleaned. First, the specimens are immersed in a 97% sulfuric acid (H_2SO_4) solution for 10 min to remove contaminants. Then, they are immersed in a 40 wt% hydrofluoric acid (HF) solution for 10 min to remove primary oxides. Finally, they are rinsed with deionized water for 10 min and dried with pure nitrogen (N_2). When preparing the electrolyte solution, the solvent is deionized water, and the electrolyte is analytical grade sodium chloride (NaCl) at a concentration of 1 wt%. This specific concentration was chosen as a compromise: it provides sufficient ionic conductivity to initiate and sustain stable microarc discharges, while avoiding the excessive current density and potential arc damage associated with higher concentrations. During mechanical polishing, a 30 wt% CeO_2 polishing solution is used, with an average abrasive particle diameter of 10 nm. The 30 wt% concentration represents a standard, high-load formulation in CMP to ensure a high rate of oxide layer removal, while the nano-scale particles are selected to prevent scratching and achieve atomic-level surface smoothness. The specimens are subjected to microarc plasma oxidation and ultrasonic-assistance microarc plasma oxidation, respectively, and then the oxide layer is removed by mechanical action.

4. Results and Discussion

4.1. Surface Components After Oxidation

The XPS (X-ray photoelectron spectroscopy) multi-functional photoelectron energy spectrometer is used to study the composition content and chemical bond states of the SiC surface. Figure 6 shows the full spectra of the 4H-SiC surface in different states.

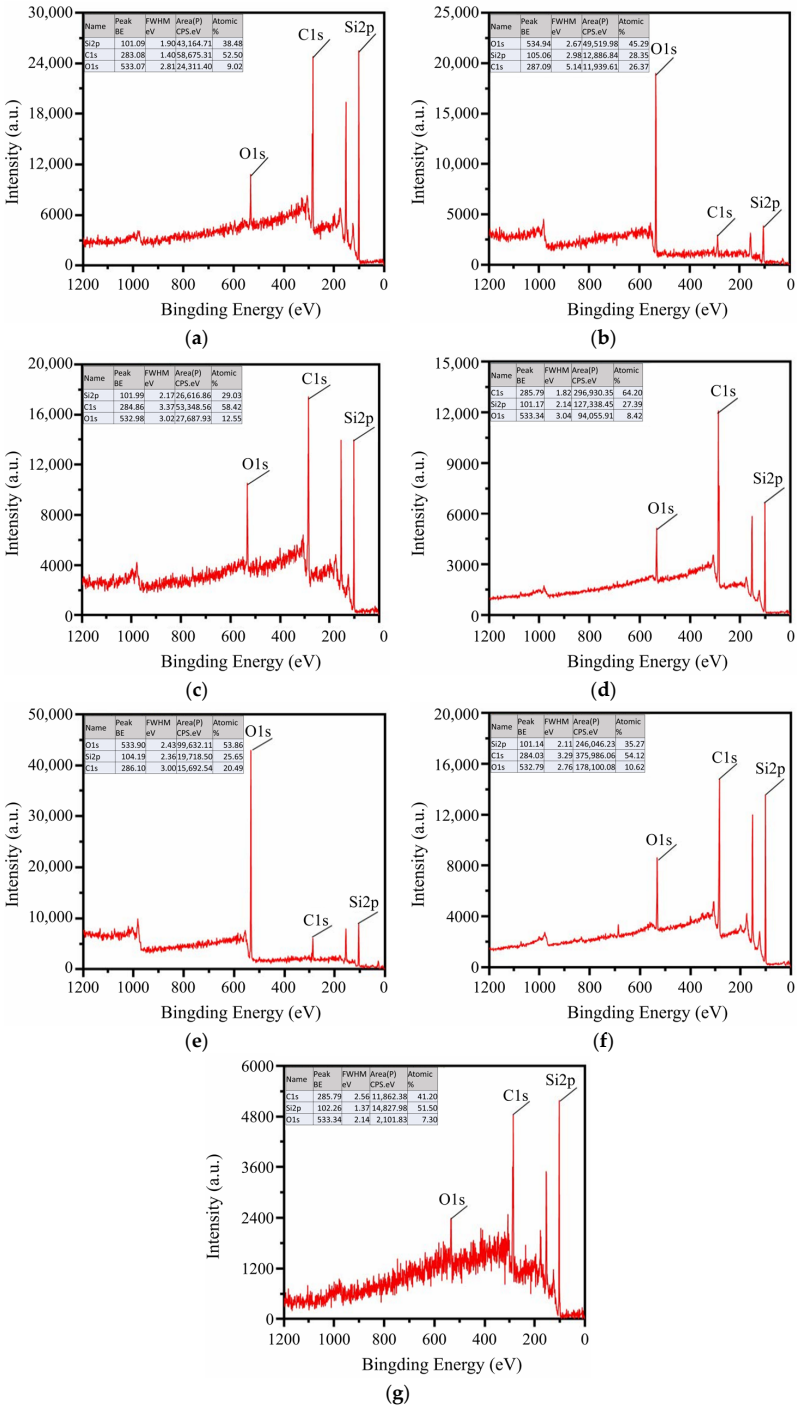


Figure 6. The full spectra of the 4H-SiC surface in different states. (**a**) Original sample. (**b**) MPO. (**c**) MPO + HF. (**d**) MPO + HF + mechanical removal. (**e**) UMPO. (**f**) UMPO + HF. (**g**) UMPO + HF + mechanical removal.

Figure 6a is the surface after chemical cleaning of the original sample. Figure 6b is the surface after microarc plasma oxidation (MPO) at 200 V for 30 s. Figure 6c is the surface after MPO at 200 V for 30 s followed by HF etching for 5 min. Figure 6d is the surface after MPO at 200 V for 30 s followed by HF etching for 5 min and then mechanically polished with 30% CeO_2 polishing solution. Figure 6e is the surface after UMPO at 200 V for 30 s. Figure 6f is the surface after UMPO at 200 V for 30 s followed by HF etching for 5 min. Figure 6g is the surface after UMPO at 200 V for 30 s followed by HF etching for 5 min and then polished with 30% CeO_2 polishing solution.

As shown in Figure 6, all the surfaces contain three elements: C, Si and O. After chemical cleaning (Figure 6a) and mechanical polishing (Figure 6d,g), the content of O is extremely low. These O elements are not the inherent components of the sample but are a layer of carbon-containing substances formed on the surface of the sample due to its exposure to the air. This substance may consist of polymer hydrocarbons, or it may be CO or CO_2.

By comparing Figure 6a with Figure 6b, it can be seen that the O content on the surface of 4H-SiC after conventional oxidation increased from 9.02% to 45.29%, indicating that after MPO, a layer of oxide is formed on the surface of the 4H-SiC. After soaking the 4H-SiC that has undergone UMPO in the HF solution for 5 min, it can be observed that the O content has decreased to 12.55%, but the O content on this surface is still higher than that of the surface after mechanical polishing shown in Figure 6d. Since HF can only dissolve SiO_2 but not SiC_xO_y, it indicates that the oxide layer formed on 4H-SiC after MPO not only contains SiO_2 but also contains SiC_xO_y. Moreover, SiO_2 is located at the top layer, while SiC_xO_y is at the bottom of the oxide layer. Comparing Figure 6b,e, after applying ultrasonic vibration, the O content of the oxide layer on the SiC surface UMPO increased from 45.29% to 53.86%, indicating that ultrasonic vibration can promote MPO and enhance the oxidation efficiency. From Figure 6c,f, it can be seen that after surface treatment with HF solution, the O content of the workpieces that underwent UMPO (10.62%) is lower than that of those underwent MPO (12.55%), suggesting that ultrasonic vibration can promote the formation of SiO_2 from SiC_xO_y, which is beneficial for subsequent mechanical polishing.

Figure 7 shows the Si2p spectrum of the surface of 4H-SiC before and after experiments. As shown in Figure 7b,e, under the conditions of a voltage of 200 V and a NaCl concentration of 1 wt%, after 30 s of either MPO or UMPO, a strong peak corresponding to the Si-O bond and a weak peak corresponding to the Si-C-O bond appear, respectively. However, in the original surface shown in Figure 7a, there is only a peak corresponding to the Si-C bond. Since the thickness of the oxide layer (including SiO_2 and SiC_xO_y) exceeds the photoelectron escape depth (<10 nm) in XPS measurements [20], no Si-C bonds are observed in Figure 7b,e. This indicates that after the 4H-SiC surface is subjected to microarc plasma oxidation and ultrasonic microarc plasma oxidation, a modified layer mainly composed of SiO_2 and a small amount of SiC_xO_y is formed on the surface. After calculation, the area ratios (i.e., content ratios) of the peaks corresponding to Si-O and Si-C-O bonds in Figure 7b,e are 2.5 and 4, respectively. This indicates that the content of SiO_2 in the oxide layer formed by UMPO is higher than that of MPO. Thus, it can be concluded that ultrasonic vibration can promote the oxidation of SiC_xO_y to SiO_2 and also shows that ultrasonic vibration can effectively promote the microarc plasma oxidation of SiC. The surface Si2p spectra of the oxidation specimens after being etched by HF solution for 5 min are shown in Figure 7c,f, respectively. In both figures, no peaks corresponding to Si-O bonds are observed, but strong peaks corresponding to Si-C bonds and weak peaks corresponding to Si-C-O bonds are present. This indicates that the SiO_2 in the oxide layer has been removed by HF, while SiC_xO_y is insoluble in HF. The area ratios (i.e., content ratios) of the corresponding peaks for Si-C and Si-C-O bonds in Figure 7c,f are 4.35 and 13.71, respectively. This indicates that the content of SiC_xO_y in the oxide layer formed by UMPO is less than that of MPO, which is beneficial for subsequent mechanical polishing. Continue with the mechanical polishing using the polishing solution containing CeO_2 abrasive for 5 min. The Si2p spectra of the surface are shown in Figure 7d,g, respectively. All the peaks corresponding to Si-O bonds and Si-C-O bonds have disappeared, and only a strong peak corresponding to Si-C bond can be observed. This result indicates that the oxide layer in Figure 7c,f has been completely removed by the CeO_2 abrasive. Moreover, SiO_2 is located at the top layer, and SiC_xO_y is located at the bottom layer of the oxide layer.

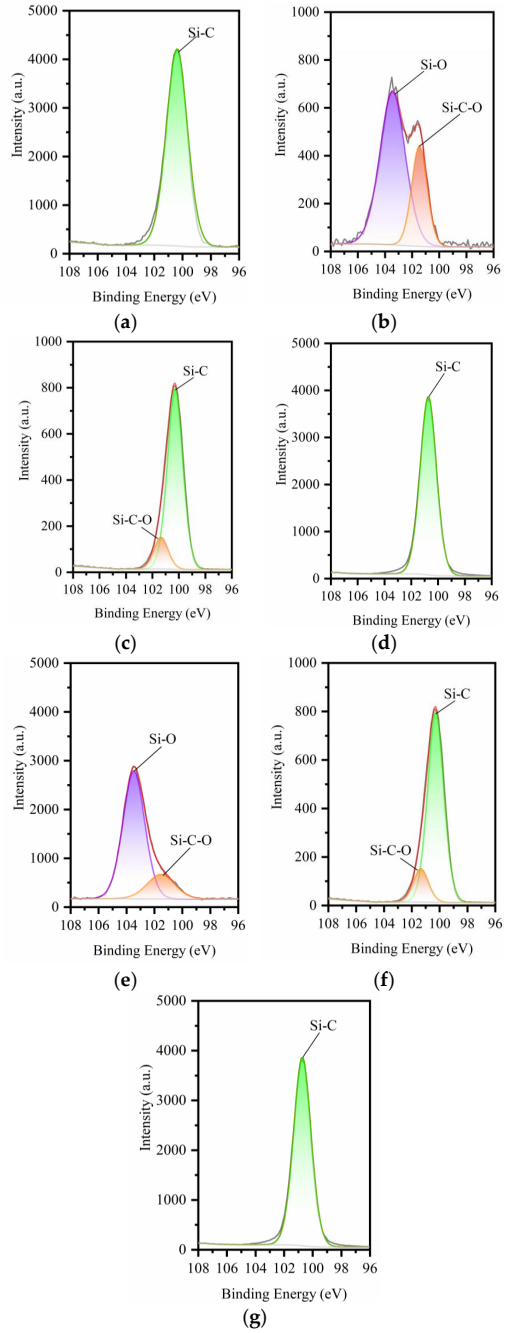


Figure 7. Si2p analysis of 4H-SiC surface. (**a**) Original sample. (**b**) MPO. (**c**) MPO + HF. (**d**) MPO + HF + mechanical removal. (**e**) UMPO. (**f**) UMPO + HF. (**g**) UMPO +HF+ mechanical removal.

4.2. The Surface Morphology After Polishing

Figure 8 shows the cross-sectional view of the 4H-SiC oxide layer after 30 s of MPO at 200 V voltage without and with ultrasonic vibration. The top layer is the carbon layer, the middle layer is the oxide layer, and the bottom layer is the 4H-SiC substrate. During the FIB sample preparation process, in order to protect the original surface of the specimen from being damaged, a layer of carbon is sprayed on the specimen surface. In Figure 8a, the thickness of the oxide layer without ultrasonic vibration is approximately 0.28 μm, while in Figure 8b, the thickness of the oxide layer with ultrasonic vibration is approximately 2.5 μm. The oxide layer with ultrasonic vibration is significantly thicker than that without ultrasonic vibration. The oxide layer after ultrasonic treatment shows obvious layering, and the internal structure of the oxide layer demonstrates that it has a porous structure.

Ultrasonic vibration can promote more active substances to pass through this porous structure and reach the oxide layer interface to oxidize the SiC substrate, thereby increasing the microarc plasma oxidation rate of the SiC.

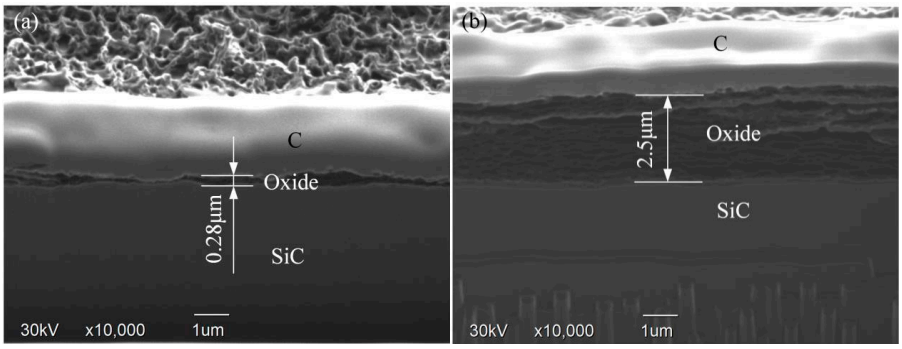


Figure 8. Cross section views of SiC surface after oxidation. (**a**) Cross section with MPO. (**b**) Cross section with UMPO.

As can be seen from Figure 9, after UMPO, the surface hardness of SiC decreased significantly from 2891.03 HV to 72.61 HV, a reduction of 39.82 times. The results show that UMPO is a very effective method for surface modification of SiC. The surface after UMPO is softer than the original surface, so it can be efficiently mechanically removed by some soft abrasive particles, thereby improving the overall polishing efficiency.

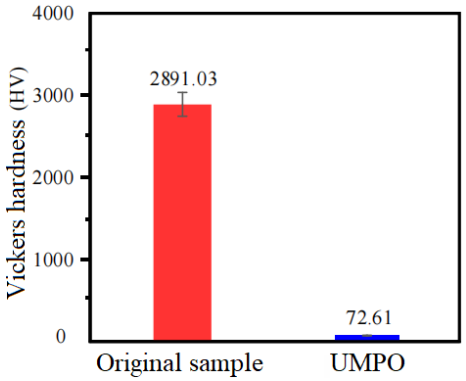


Figure 9. Vickers hardness of the UMPO oxide layer.

After being oxidized for 5 min under different oxidation voltages, and then mechanically polished for another 5 min, the SEM surface morphology of the 4H-SiC is shown in Figure 10. Regardless of whether ultrasonic vibration is applied or not, the surface defects are least at 200 V. The incomplete removal of defects is due to insufficient oxidation time, resulting in incomplete oxidation of the defective surface. Therefore, after removing the oxide layer, there are still pits and shallow scratches on the surface, but the overall quality is significantly improved compared to the original surface. When the voltage is 350 V, all the surface scratches disappear after the oxide layer is removed, but there are a large number of pits. This is because the voltage at this time exceeded the voltage value of the MPO area, causing arc discharge. The excessive discharge energy led to a high oxidation rate, and thus the defective surface is completely oxidized. However, arc discharge would cause damage to the surface of the workpiece, resulting in new surface damage. Additionally, regardless of the voltage, the surface quality after applying ultrasonic vibration is significantly better than that without ultrasonic vibration, indicating that the addition of ultrasonic vibration enables more surface defects to be oxidized, thereby improving the surface quality after polishing.

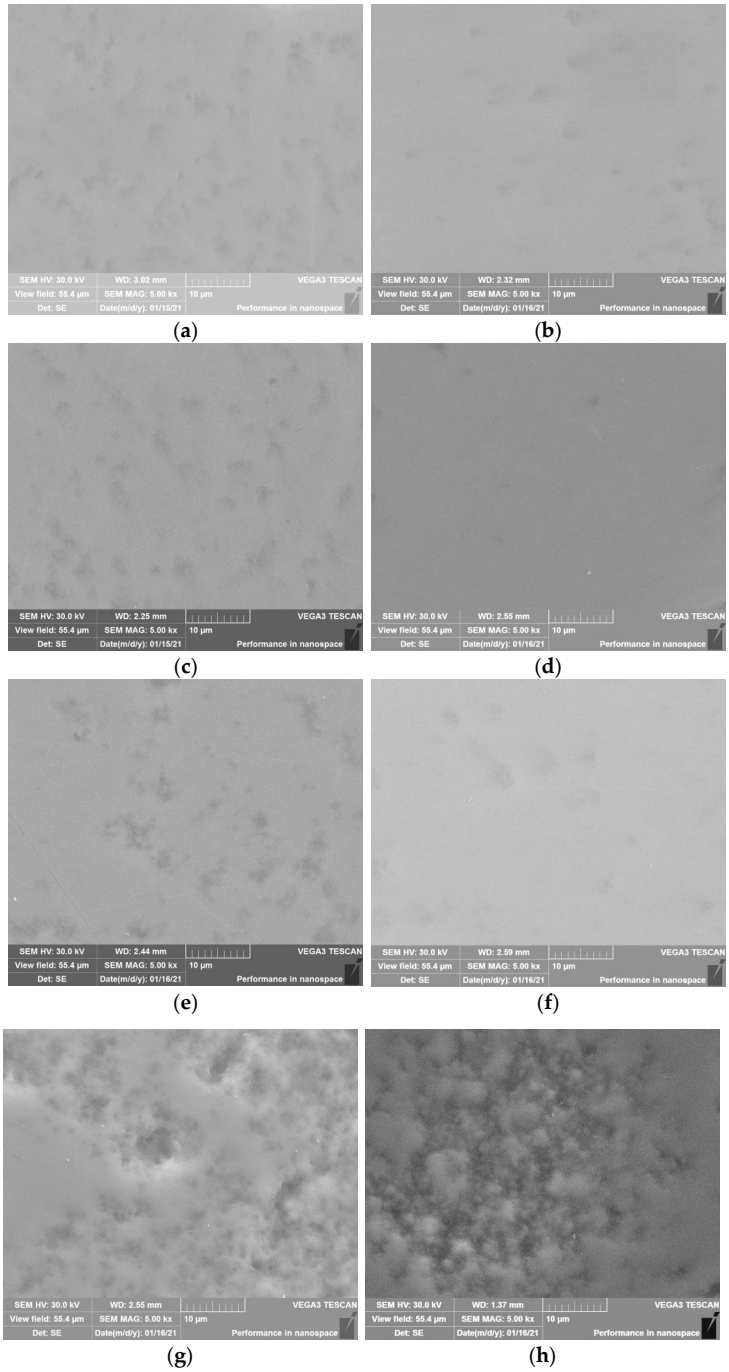


Figure 10. SEM images of 4H-SiC under different states after polishing. (**a**) 150 V MPP. (**b**) 150 V UMPP. (**c**) 200 V MPP. (**d**) 200V UMPP. (**e**) 250 V MPP. (**f**) 250 V UMPP. (**g**) 350 V MPP. (**h**) 350 V UMPP.

After being oxidized for 5 min under different oxidation voltages, then mechanically polished for 5 min, the three-dimensional morphology of the SiC SWLI surface is shown in Figure 11. In both situations (with or without ultrasonic vibration), compared with the original SiC surface before oxidation shown in Figure 11a, the surface quality after polishing is significantly higher, and the surface roughness is greatly reduced. Among them, the surface roughness at 200 V is the lowest. When the voltage is 350 V, although all the scratches on the surface after oxidation layer's removal disappeared, there are deep pits. The fitting on the SiC surface is because, at this high voltage, it exceeds the voltage value of the microarc oxidation area and transforms into arc discharge, with excessive discharge energy, burning the surface of the workpiece to form the fitting. Additionally, regardless of the voltage, the surface roughness after applying ultrasonic vibration is significantly lower

than that without ultrasonic vibration, indicating that ultrasonic vibration improved the oxidation efficiency, which is consistent with the conclusion in Figure 10.

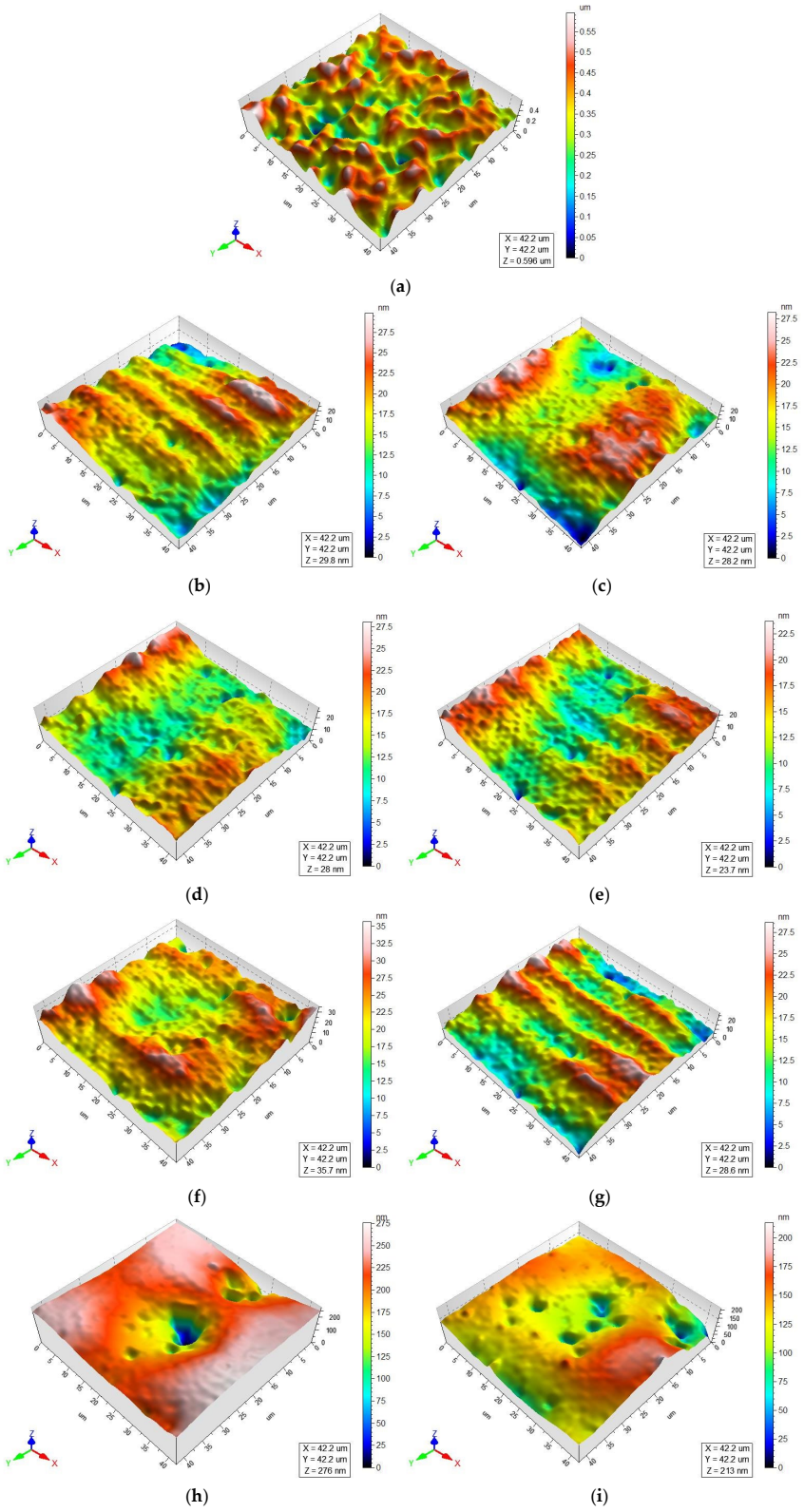


Figure 11. SWLI images of 4H-SiC under different voltages after polishing. (**a**) Original sample, Ra = 55.3 nm. (**b**) 150 V MPP, Ra = 1.22 nm. (**c**) 150 V UMPP, Ra = 0.86 nm. (**d**) 200 V MPP, Ra = 0.75 nm. (**e**) 200 V UMPP, Ra = 0.54 nm. (**f**) 250 V MPP, Ra = 0.89 nm. (**g**) 250 V UMPP, Ra = 0.73 nm. (**h**) 350 V MPP, Ra = 11.2 nm. (**i**) 350 V UMPP, Ra = 7.96 nm.

4.3. Material Removal Rate and Surface Roughness

Experiments are conducted to investigate the microarc plasma polishing of 4H-SiC under different oxidation voltages with or without ultrasonic vibration. The 1 wt% NaCl electrolyte is used, and the oxidation voltages are 50 V, 100 V, 150 V, 200 V, 250 V, 300 V, and 350 V, whose f = 20 kHz, D = 50%. After oxidation for 5 min, the oxide layer is removed by mechanical polishing with 30 wt% CeO_2.

The height difference between the polished area and the original wafer at the boundary could be measured using a white light confocal microscope to obtain the material removal height of 4H-SiC, dividing by the oxidation time gives the oxidation rate, shown in Figure 12. The material removal rate (MRR) can be further obtained through Equation 12. The surface roughness Ra after polishing can also be measured using a white light confocal microscope.

$$MRR = h/(t_0 + tm) \tag{12}$$

where h is the measured oxidation film height, t_0 is the oxidation time, t_m is the mechanical polishing time.

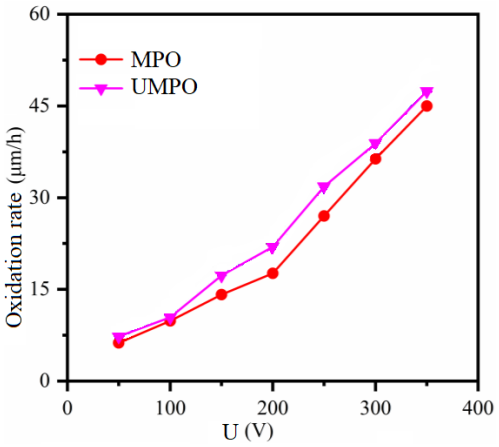


Figure 12. Oxidation rate with different voltages.

The experimental results are shown in Figure 13. It can be seen that the oxidation rate increases with the increase of voltage. The surface roughness after polishing first decreases and then increases with the increase of voltage, reaching the minimum at 200 V. Because under these experimental conditions, the area around 200 V is the most suitable for 4H-SiC's microarc plasma oxidation, and the surface modification in this area is suitable for surface flattening. 250 V and 300 V are in the arc transition zone. The gas ionization rate in this area is higher than that in the microarc discharge zone, and occasional spark discharge occurs, so the surface quality after polishing decreases. At 350 V, it is located in the arc discharge zone, where the gas ionization rate is the highest. The arc discharge generated here will burn the surface of the workpiece, resulting in the poorest surface quality after polishing. After applying ultrasonic vibration, the oxidation rate of the SiC increases, and the surface roughness decreases after the oxide layer is removed. This indicates that ultrasonic vibration can enhance the oxidation rate, thereby improving the surface quality after polishing. When U = 200 V, oxidation for 5 min with ultrasonic vibration, after mechanical polishing, the smoothest surface with a Ra value of 0.54 nm can be obtained. At this point, the material removal rate is 21.7 μm/h. Compared to that without ultrasonic vibration, the surface roughness is reduced by 28%, and the material removal rate is increased by 21.9%.

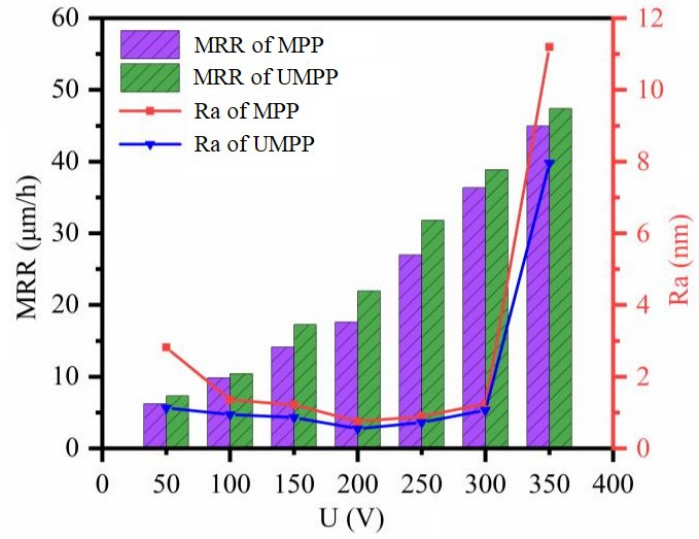


Figure 13. Relationship between MRR & Ra with different voltages.

5. Conclusions

Aiming at the problem of poor surface quality and low material removal rate of 4H-SiC's polishing, this paper establishes an ultrasonic-assistance microarc plasma polishing (UMPP) method for SiC. The related mechanism is analyzed, and experiments are carried out. The specific conclusions are as follows:

Based on the properties of microarc plasma and the theory of gas discharge, the mechanism of the SiC microarc plasma oxidation and the ultrasonic enhancement mechanism are analyzed. During the microarc plasma oxidation process, the gas layer on the surface of the workpiece is broken through by high-energy pulse power supply, generating a plasma gas layer; the strong oxidizing hydroxyl radicals (•OH) produced by charge transfer and collision in the plasma gas layer oxidized 4H-SiC, resulting in the formation of an oxide layer. The oxide layer contains SiO_2 on the outer layer and a small amount of SiC_xO_y on the inner layer.

The ultrasonic vibration activates the discharge frequency and energy of the surface plasmonic gas layer of the 4H-SiC through thermal effect, acoustic effect and chemical effect, accelerates the generation rate of hydroxyl radicals (•OH), and increases the oxidation rate of SiC. The component analysis of the oxide layer in the experimental results also further proves that ultrasonic vibration can promote the microarc plasma oxidation process and improve the surface quality after polishing. At the same time, it promotes the generation of more amorphous layers, which is beneficial for the subsequent mechanical removal process of the oxide layer and improves the material removal rate.

The proposed ultrasonic-assistance microarc plasma polishing method for 4H-SiC in this paper is an efficient and high-quality polishing method for SiC. Experimental results show that the oxidation rate increases with the increase of voltage, and the surface roughness after polishing first decreases and then increases, reaching the minimum at 200 V. Under these experimental conditions, the 200 V range is the most suitable micro-arc discharge area for the plasma oxidation of 4H-SiC electrolyte, and the surface modification in this area is suitable for surface flattening. When U = 200 V, ultrasonic-assisted oxidation for 5 min followed by mechanical polishing can obtain the smoothest surface with Ra = 0.54 nm. At this time, the material removal rate is 21.7 μm/h. Compared with no ultrasonic assistance, the surface roughness is reduced by 28%, and the material removal rate is increased by 21.9%.

Author Contributions: Conceptualization, F.L. and J.Y.; methodology, J.Y. and S.L.; validation, investigation, J.S., Z.Y. and Y.Z.; writing—original draft preparation, F.L.; writing—review and editing, J.Y.; supervision, Z.Y. All authors have read and agreed to the published version of the manuscript.

Funding: This research was funded by Shaanxi Provincial Department of Education Natural Science Youth Project (21JK0806), University Engineering Research Center Project of Education Department of Shaanxi Province (24JR118) and Key Research and Development Projects of Shaanxi Province (2021GY-275).

Data Availability Statement: The original contributions presented in this study are included in the article. Further inquiries can be directed to the corresponding author.

Acknowledgments: The author is sincerely grateful to all co-authors for their invaluable theoretical contributions and steadfast support throughout this work.

Conflicts of Interest: The authors declare no conflicts of interest.

References

1. Lin, C.; Xie, J.; Lu, J.; Yan, Q. Study on the effect of process parameters and removal behavior of single-crystal SiC polishing based on a photocatalytic fixed polishing plate. *Diam. Relat. Mater.* **2025**, *153*, 111985. [CrossRef]
2. Wang, Z.; Zhu, Y.; Ren, R.; Zhang, T.; Peng, Y.; Wang, Y.; Lu, X.; Wang, C. Insight into the atomic-scale material removal of 4H-SiC electrochemical mechanical polishing (ECMP) using graphene oxide. *Tribol. Int.* **2025**, *210*, 11083. [CrossRef]
3. Kang, H.; Zhong, M.; Li, X.; Yi, M.; Chen, J.; Xu, W. Investigation of Fenton-electrochemical oxidation behavior and polishing mechanism of SiC. *Precis. Eng.* **2025**, *93*, 334–343. [CrossRef]
4. Shen, M.; Wei, M.; Wu, L.; Han, Y.; Hong, B.; Lyu, B.; Chen, H.; Hang, W. Dominant parameters and mechanisms influencing the electrochemical shear-thickening polishing of 4H-SiC. *Ceram. Int.* **2025**, *51*, 10351–10364. [CrossRef]
5. Zhao, Y.; Gao, S.; Sun, Y.; Wu, Y.; Yang, F.; Kang, R.; Dong, Z. Electric-field-modulated oxidation and its effect on photoelectrochemical mechanical polishing of 4H-SiC. *Int. J. Mech. Sci.* **2025**, *295*, 110247. [CrossRef]
6. Li, C.; Shen, M.; Li, X.; Fu, Y.; Dong, Y.; Lyu, B.; Yuan, J. Chemical-mechanical polishing of 4H-SiC using multi-catalyst synergistic activation of potassium peroxymonosulfate. *Processes* **2025**, *13*, 1094. [CrossRef]
7. Gao, S.; Hu, B.; Song, X.; Dong, Z.; Kang, R. Dispersal mechanism of different dispersants and its effect on performance of 4H-SiC polishing slurry. *Ceram. Int.* **2025**, *51*, 3943–3952. [CrossRef]
8. Feng, K.; Xu, L.; Gu, Y.; Zhao, L.; Zhao, T.; Lyu, B. Study on material removal mechanism of solid phase Fenton catalytic polishing of SiC wafer with gel-forming abrasive disc. *Mater. Sci. Semicond. Process.* **2025**, *194*, 109488. [CrossRef]
9. Zhu, R.; Zhang, T.; Yao, Q.; Peng, Y.; Cheng, F.; Wang, Z.; Wang, Y.; Lu, X.; Wang, C.; Zhao, Y. Atomistic mechanisms of SiC electrochemical mechanical polishing in aqueous H_2O_2: A ReaxFF molecular dynamics study. *J. Manuf. Process.* **2025**, *136*, 56–67. [CrossRef]
10. Hu, Y.; Shi, D.; Hu, Y.; Zhao, H.; Sun, X. Investigation on the material removal and surface generation of a single crystal SiC wafer by ultrasonic chemical mechanical polishing combined with ultrasonic lapping. *Materials* **2018**, *11*, 2022. [CrossRef] [PubMed]
11. Chen, X.; Liang, Y.; Cui, Z.; Meng, F.; Zhang, C.; Chen, L.; Yu, T.; Zhao, J. Study on material removal mechanism in ultrasonic chemical assisted polishing of silicon carbide. *J. Manuf. Process.* **2022**, *84*, 1463–1477. [CrossRef]
12. Li, J.; Geng, D.; Zhang, D.; Qin, W.; Jiang, Y. Ultrasonic vibration mill-grinding of single crystal silicon carbide for pressure sensor diaphragms. *Ceram. Int.* **2018**, *44*, 3107–3112. [CrossRef]
13. Chen, G.; Pan, L.; Luo, H.; Zhou, Y.; Luo, G.; Pan, G. Chemical mechanical polishing of silicon carbide (SiC) based on coupling effect of ultrasonic vibration and catalysis. *J. Environ. Chem. Eng.* **2023**, *11*, 111080. [CrossRef]
14. Chen, X.; Zhang, C.; Meng, F.; Yu, T.; Zhao, J. Polishing mechanism analysis of silicon carbide ceramics combined ultrasonic vibration and hydroxyl. *Tribol. Int.* **2023**, *179*, 108187. [CrossRef]
15. Mi, T.; Jiang, B.; Liu, Z.; Fan, L. Plasma formation mechanism of microarc oxidation. *Electrochim. Acta* **2014**, *123*, 369–377. [CrossRef]
16. Koshuro, V.A.; Fomin, A.A.; Rodionov, I.V.; Fomina, M.A. The Effect of Microarc Oxidation on the Structure and Hardness of Aluminum-Oxide Coatings Formed by Plasma Spraying on Titanium. *Prot. Met. Phys. Chem. Surf.* **2018**, *54*, 840–844. [CrossRef]
17. Zhao, Q.; Yang, H.; Li, G.; Liu, Z. Structure and properties of a bioactive coating on zirconium produced by microarc oxidation. *Mater. Technol.* **2017**, *32*, 191–195. [CrossRef]
18. Danilov, I.; Hackert, M.; Zinecker, M.; Meichsner, G.; Edelmann, J.; Schubert, A. Process understanding of plasma electrolytic polishing through multiphysics simulation and inline metrology. *Micromachines* **2019**, *10*, 214. [CrossRef] [PubMed]

19. Jiang, B.; Li, J. Engineering Application of Micro-Arc Oxidation Treatment Technology for Aluminum-Magnesium Alloys. *New Technol. New Process.* **2009**, *02*, 16–18. [CrossRef]
20. Deng, H.; Yamamura, K. Atomic-scale flattening mechanism of 4H-SiC (0001) in plasma assisted polishing. *CIRP Ann.* **2013**, *62*, 575–578. [CrossRef]

Disclaimer/Publisher's Note: The statements, opinions and data contained in all publications are solely those of the individual author(s) and contributor(s) and not of MDPI and/or the editor(s). MDPI and/or the editor(s) disclaim responsibility for any injury to people or property resulting from any ideas, methods, instructions or products referred to in the content.